J Fusion Energ (2010) 29:553–557
DOI 10.1007/s10894-010-9327-6

ORIGINAL RESEARCH

Formation of High-β ECH Plasma and Inward Particle Diffusion in RT-1

H. Saitoh · Z. Yoshida · J. Morikawa · Y. Yano · T. Mizushima · M. Kobayashi

Published online: 6 September 2010

Abstract High-β plasma is stably confined in the Ring Trap 1 (RT-1) device, a magnetospheric configuration with a levitated dipole field magnet. The plasma pressure is mainly resulted from high temperature electrons generated by electron cyclotron resonance heating (ECH), whose bremsstrulung was observed by an X-ray CCD camera. The coil support structure is the main loss route of the hot electrons, and higher-β discharge is realized by coil levitation. Confinement properties of charged particles in the magnetospheric configuration were investigated by using toroidal non-neutral plasma. Fluctuation-induced inward particle diffusion into the strong magnetic field region was realized due to the onset of diocotron (Kelvin–Helmholtz) instability.

Keywords Magnetospheric configuration · Dipole confinement · High-β plasma · Non-neutral plasma

Introduction

The Ring Trap 1 (RT-1) device [1] was constructed aiming for the confinement of high-β plasma in a magnetospheric configuration suitable for burning advanced fusion fuels [2–4]. The magnetic configuration of RT-1 is similar to the Jovian magnetosphere, where high-β flowing plasma is observed. A two-fluid relaxation theory predicts an ultra high-β state (possibly exceeds 1) realized by the effects of hydrodynamic pressure when the plasma has an Alfvénic fast flow [5]. RT-1 has started plasma experiment in 2006 and succeeded to stably produce plasma with magnetic coil levitation [6]. Formation of toroidal flow and evaluations of its effects are not conducted in the present experiment. In this paper, we report the recent experimental progress of RT-1, including the formation of high-β plasma by ECH and its imaging by a soft X-ray CCD camera [7], and stable confinement and inward particle diffusion of pure electron plasma [8].

H. Saitoh (✉) · Z. Yoshida · J. Morikawa · Y. Yano · T. Mizushima · M. Kobayashi
Graduate School of Frontier Sciences, University of Tokyo, 5-1-5 Kashiwanoha, Kashiwa, Chiba 277-8561, Japan
e-mail: saito@ppl.k.u-tokyo.ac.jp

Experimental Setup

RT-1 generates a magnetospheric configuration by a superconducting magnet (Fig. 1). Inside the chamber of RT-1, a dipole field coil made with Bi-2223 high-temperature superconducting wires is magnetically levitated. The coil is cooled down to 20 K by GM refrigerators, and 6 h of coil levitation experiment is carried out before the coil temperature rises to 30 K. The superconducting magnet and a levitation magnet are operated with permanent current of 250 and 28.8 kAT. The plasma is generated by ECH using 2.45 GHz (20 kW) and 8.2 GHz (25 kW) microwaves. More detailed explanation of RT-1 is in Ref. [1].

The diagnostic system of RT-1 includes magnetic loops, fast magnetic probes, edge Langmuir probes, a 75 GHz interferometer, a visible light spectroscopy, soft X-ray photodiodes, and a soft X-ray CCD camera. Four magnetic loops (three turns each) are winded outside of the chamber at $r = 101$ cm. The loops were located at $z = \pm 20$ cm and $z = \pm 35$ cm. For the present plasma pressure range, we found an empirical relation between the averaged diamagnetic signal $\Delta\Phi$ and maximum local β: $\beta[\%] \sim 18 \times \Delta\Phi$ [mWb], by Grad–Shafranov equilibrium analysis. A 75 GHz ($\lambda = 4$ mm) interferometer is installed for the

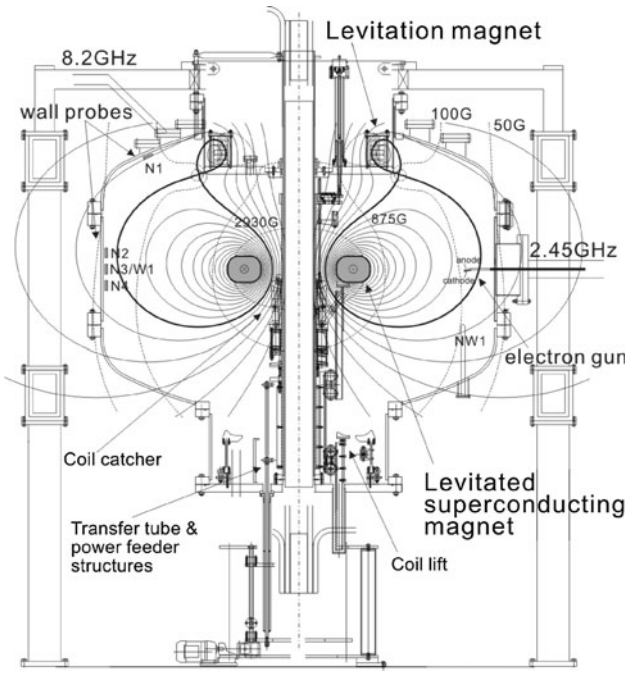

Fig. 1 Cross section of RT-1 including coil magnets, vacuum chamber, and RF waveguides. Thin lines show magnetic surfaces and field strengths

measurements of electron line density n_l. The transmitter and receiver of the interferometer were placed at the north and south tangential ports with quartz viewports, and the length between the each port is 1.78 m. When the plasma is distributed inside the separatrix of the vacuum magnetic field generated by the combination of the levitated and levitation coils, path length of the microwave inside the plasma is 1.6 m. We use this value for the calculation of averaged electron density: $n_{ave} = n_l/1.6$. Assuming a radially parabolic density profile $n_e(r) = n_{peak} \times [1-4\ (r-0.5)^2]$ with peak density n_{peak} at $r = 0.5$ m (near the ECR layer), the line integrated density n_l is related with n_{peak} as $n_l = 1.36 n_{peak}$.

High-β Plasma Formation and X-ray Imaging

The ECH-generated plasma in RT-1 has multiple electron populations with different temperatures. By optimizing filling neutral gas pressure below approximately 10 mPa, decrease in visible light strength and increase in diamagnetic loop signal and X-ray signals are observed (Fig. 2), as ECH generates considerable ratio of hot electrons. Soft X-ray measurements using Si(Li) detectors show that the hot electron component is in the temperature range of 1–50 keV. The hot electron component has relatively long confinement time due to its small cross section of ionizing collisions with neutrals. The maximum decay time of n_l

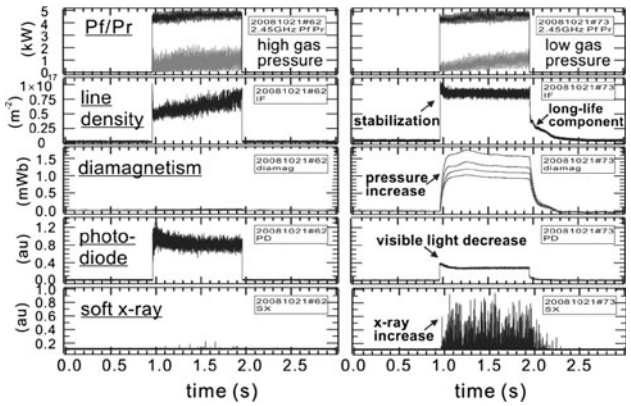

Fig. 2 Typical waveforms with filling hydrogen pressure of 45 mPa (*left*) and 1.3 mPa (*right*)

after RF is turned off is observed to be 0.9 s. Edge Langmuir probe measurement shows that the cold electrons have temperatures of around 10 eV. The total maximum energy confinement time estimated from the stored energy measured by magnetic loops and injected RF power is $\tau_e \sim 60$ ms with an electron density of $1 \times 10^{17} m^{-3}$.

Figure 3 shows diamagnetic loop signals and n_l measured by the interferometer. The electron density with 2.45 GHz ECH exceeds the O-mode cut off density, suggesting mode conversion to the electron Bernstein wave. For the similar input RF power, higher stored energy is realized with 2.45 GHz discharge in the initial phase of experiments, as shown in the figure. In this phase, plasma generated by 8.2 GHz RF mainly consists of cold electrons and has relatively low pressure. Discharge cleaning and even repeated plasma production drastically improves the pressure of plasma especially when generated by 8.2 GHz RF. Figure 4 shows the parameters of plasma generated in succession with same conditions. Reduction of gas pressure during discharge, and increase in T_e (not shown in the figure) and the ratio of hot component were simultaneously observed, resulting the improved plasma performance. Temporal variation of hydrogen gas pressure depends on

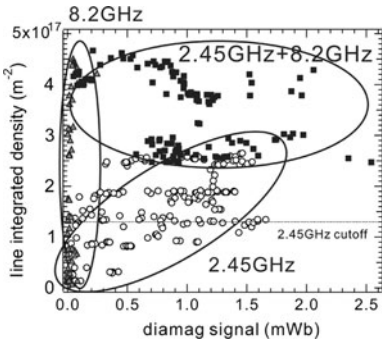

Fig. 3 Diamagnetic loop signal and line integrated density for discharges with different RF frequencies

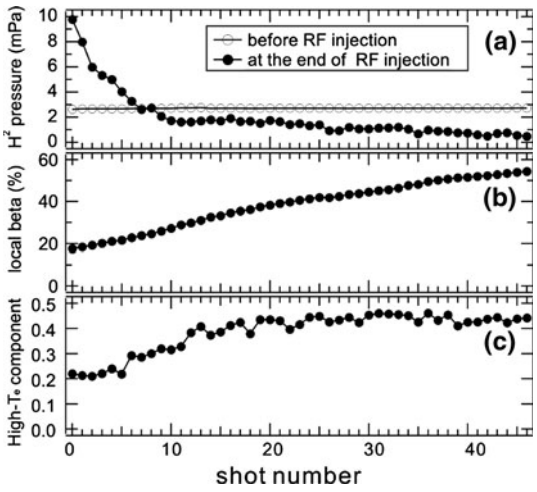

Fig. 4 **a** Hydrogen gas pressure before and during plasma production, **b** maximum local β, and **c** ratio of hot (*slow decay*) component electrons with repeated 8.2 GHz RF injection

the particle balance in the vacuum chamber. It is probable that the effects of gas recycling are intensive for cases with 8.2 GHz RF, because the resonance layer of ECH (2930G line in Fig. 1) intersects the superconducting coil and the generated hot electrons directly hit the coil surface. The observed temporal improvement was realized due to the reduction of stored hydrogen gas on the coil case and decreased neutral gas pressure.

For direct measurements of the spatial profiles of the hot electrons, or pressure profiles of the plasma, we installed a soft X-ray CCD camera in RT-1 [7]. Figure 5 shows the top view of RT-1 including the camera ports, a visible light image from port 1, and X-ray images. When 8.2 GHz RF is applied, where the ECR layer intersects the case of the dipole field coil, X-ray emitting region is localized near the coil (Fig. 5d). Bremsstrahlung caused by the collisions between the energetic electrons and the coil case is also observed, indicating that some of the hot electrons with large Larmor radii are lost before filling the confinement region. For 2.45 GHz discharges in Fig. 5c, X-rays are observed over approximately entire region inside the image circle of the camera. These observations agree with the measurements of magnetic loops; the plasma pressure for 2.45 GHz RF experiments is relatively higher than those with 8.2 GHz RF. When the coil is not levitated, the major loss channel of the hot electrons is the support structure of the coil as shown in Fig. 5e.

Levitation of the superconducting coil results typically factor 2 or 3 improvements of the electron density and plasma pressure, and the maximum local β value in recent experiment is approximately 70%. An X-ray image of plasma with levitated coil and enhanced performance is shown in Fig. 5f. As plasma pressure increases, the shape of magnetic separatrix expands outward, and some hot

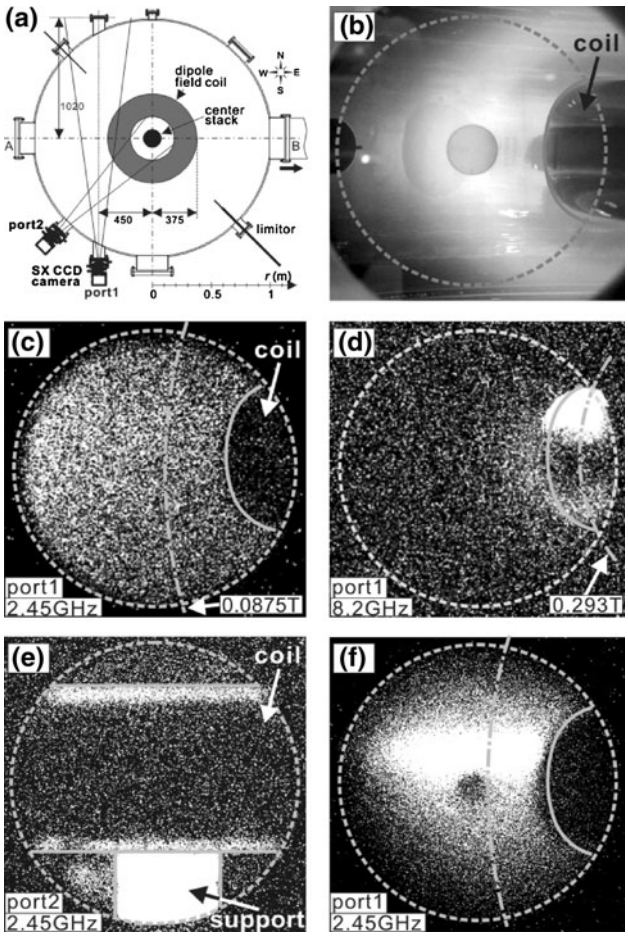

Fig. 5 **a** Top view of RT-1 including X-ray camera port 1 and 2, and **b** visible light image from port 1. Typical X-ray images of (**c–e**) moderate-β plasma generated by 2.45 and 8.2 GHz ECH with supported coil and **f** high-β plasma generated by 2.45 GHz with coil levitation

electrons hit the chamber wall as shown in the figure. The dark hole in the image corresponds to the concave port structure located on the chamber wall (Fig. 5a). The strongest X-ray emitting region is apart from the equator of the chamber, due to the vertical asymmetry of the separatrix.

The X-ray CCD camera has 1,024 × 1,024 pixels with 16 bit dynamic range and it can also be used for energy analysis of photons, as far as the injected X-ray flux is sufficiently small and each photon signal is separated. Figure 6 shows the energy spectrum of X-ray of the plasma generated by 2.45 GHz ECH with input RF power of 3 kW, measured by the photon counting mode of the CCD camera. The spectrum has lines of impurities derived from SUS304 stainless-steel chamber wall, and Cr Kα (5.41 keV) and Fe Kα (6.40 keV) lines are used for energy calibration. The hot electron temperature is calculated to be $T_e = 2.7$ keV, which shows good agreement with the result of the Si(Li) detector. Measurements of spatial profiles of

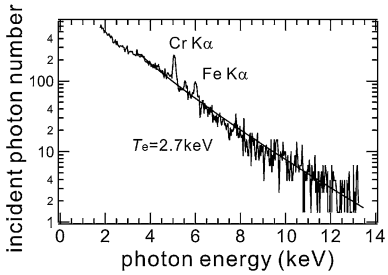

Fig. 6 X-ray energy spectrum of plasma measured by photon-counting mode of CCD camera

T_e with coil levitation are not carried out at present and it is a future task to be done.

Long Time Confinement and Inward Diffusion of Pure Electron Plasma

Confinement properties of charged particles in the magnetospheric configuration were investigated by using pure electron plasma [8]. As well as for basic studies in fusion plasmas, toroidal confinement of non-neutral plasma has potential scientific applications for charged particle traps. Because the toroidal geometry requires no plugging electric field in contrast to the linear geometries, it can trap plasmas with arbitrary non-neutrality including antimatter particles such as antihydrogen or positron–electron plasmas. Although the single particle orbit of an electron is localized near the initial magnetic surface due to the conservation of the canonical angular momentum of a charged particle, inward diffusion of particles to strong field and stable confinement of plasma are realized.

Figure 7 shows the typical waveform of the electron plasma formation in RT-1. We inject electron beam from

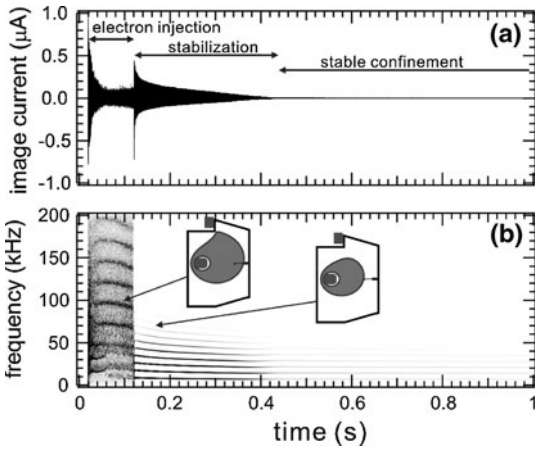

Fig. 7 **a** Electrostatic fluctuation of toroidal electron plasma and **b** its power spectrum during electron injection and stabilization phases. Estimated confinement regions are also shown

an electron gun located at the edge confinement region typically at $r_{gun} = 70$ cm into static fields, with an initial acceleration voltage of $V_{acc} \sim 200$ V. At the beginning of the beam injection and just after the injection ended, the plasma has large amplitude fluctuation. During the injection phase, multiple frequency peaks are observed. After the electron injection ended, the plasma is stabilized and long confinement is realized. The observed coherent fluctuation implies a rigid-rotor equilibrium state of the plasma, although the plasma is confined in the strongly inhomogeneous dipole magnetic field. The stable confinement time at the base pressure of RT-1 of 7×10^{-7} Pa was 320 s. This confinement time is close to the diffusion time caused by collisions of electrons with neutral molecules, and the confinement usually ends with rapid onset of instability.

For perturbation-free measurements of the spatial profiles of electron plasma, especially in the stable confinement phase, we used a wall probe array [9]. Each of the wall probe signal was monitored by a current amplifier and an integration circuit, and the strength of a radial electric field was directly measured at each of the wall. We used three wall probes and estimated the confinement regions of the plasma that most well reconstruct the wall probe measurements. Estimated plasma regions for the typical cases of during electron injection and after the electron supply ended are shown in Fig. 7b. During the electron gun operation, the outer edge of the electron confinement region approximately agreed with the magnetic separatrix. After the electron supply ended, electrons on the magnetic surfaces that intersected the electron gun structures were rapidly lost. In the stable confinement period, electrons shifted inward and moved to the strong magnetic field region. The electron density is estimated to be $\sim 10^{11}$ m^{-3}. Before the realization of stable confinement, repeated frequency drop and simultaneous instability burst and radial particle transport are observed. The observed inward diffusion indicates the violation of the third adiabatic invariant and radial diffusion of charged particle caused by perturbations with a time scale comparable to or shorter than the toroidal drift period of the plasma.

Conclusion

Stable confinement of high-β plasma is realized in RT-1. In the present experiment, the plasma is generated by 2.45 and 8.2 GHz ECH, and the plasma pressure is mainly resulted from high energy electrons. A soft X-ray CCD camera is installed in RT-1 for the measurements of spatial profiles of the hot electrons. Without coil levitation, coil support structure is the main loss channel of hot electrons, which agrees with the drastic improvements of the plasma

pressure by the coil levitation. The confinement properties of the magnetospheric configuration were studied using non-neutral plasma, and inward diffusion of charged particles was observed.

References

1. Y. Ogawa et al., Plasma Fusion Res. **4**, 020 (2009)
2. Z. Yoshida et al., 22th IAEA Fusion Energy Conference, Geneva, EX/P5-28 (2008)
3. D.T. Garnier et al., Nucl. Fusion **49**, 055023 (2009)
4. A. Hasegawa, Comm. Plasma Phys. Control. Fusion **11**, 147 (1987)
5. S.M. Mahajan, Z. Yoshida, Phys. Rev. Lett. **81**, 4863 (1998)
6. Y. Yano et al., Plasma Fusion Res. **4**, 039 (2009)
7. H. Saitoh et al., Plasma Fusion Res. **4**, 050 (2009)
8. Z. Yoshida et al., Phys. Rev. Lett. **104**, 235004 (2010)
9. H. Saitoh et al., Plasma Fusion Res. **4**, 054 (2009)